Electrical Power and Energy Systems 78 (2016) 277–284

Contents lists available at ScienceDirect

Electrical Power and Energy Systems

journal homepage: www.elsevier.com/locate/ijepes

Fault location scheme for multi-terminal transmission lines using unsynchronized measurements

Shoaib Hussain [a], A.H. Osman [b,*]

[a] Department of Electro-Mechanical Engineering Technology, Abu Dhabi Polytechnic, Abu Dhabi, United Arab Emirates
[b] Department of Electrical Engineering, American University of Sharjah, Sharjah, United Arab Emirates

ARTICLE INFO

Article history:
Received 9 October 2014
Received in revised form 22 September 2015
Accepted 17 November 2015

Keywords:
Faulted leg identification
Fault location
Multi-terminal lines
Unsynchronized measurements
Transmission line protection

ABSTRACT

In this paper, a simple alternative fault location algorithm for multi-terminal transmission lines using unsynchronized measurements is proposed. The developed data synchronization procedure is employed to identify the faulted leg before the fault location is calculated. The fault location algorithm is independent of the fault resistance and source impedance variations. The proposed faulted leg identification and location algorithm is extensively tested for all major fault types and different high fault resistances. The results show that the proposed multi-terminal fault location algorithm is fast, accurate and immune to power system transients.

Introduction

Fault location on overhead power transmission lines remains a subject of great interest and has been intensively studied over the years [1–15]. Fault locators, compared to protection relays, are expressly designed to pinpoint the exact location of faults on transmission lines to expedite the process of repair and power restoration. Multi-terminal power transmission systems such as teed-feeders (three-terminal lines) are economically and environmentally attractive. However, their protection design is challenging. Multi-terminal lines pose additional problems due to remote-end in-feeds from other connecting lines and the incident fault impedance [1–3].

Numerous schemes, which utilize the fundamental frequency of voltage and current phasors in fault detection and location, have been proposed in the literature. These algorithms can be broadly categorized as single-end measurement algorithms [4–7], two-end measurement algorithms [8–12] and multi-terminal fault location algorithms [1–3,10,15].

Two-ended measurement algorithms collect signals from both ends of a transmission line and offer superior performance compared to single-end algorithms due to their apparent insensitivity to source impedance, fault resistance and remote-end in-feed [9,11]. Additionally, signal measurements obtained for algorithm evaluation might come from time-synchronized data recorders with the aid of PMUs (Phasor Measurement Units) and GPS, or from asynchronous fault data recorders that do not share a common time Refs. [13,14].

Fault location algorithm for teed-feeders that carries out data synchronization by selecting a common reference and equating the voltages at the teed-point is proposed in [1]. Super-imposed component extraction and modal transformation is used for fault distance calculation. However, the authors assume synchronization mismatch of only a few data samples and the delivered algorithm wasn't tested for large or obtuse synchronization angles. The three-terminal protection scheme that uses Clarke transformation to decouple the inter-phase quantities and develop a fault detection index is proposed in [2]. The algorithm offers high-speed response but needs synchronized data measurement from PMUs and GPS.

A simple protection approach for multi-terminal transmission lines using synchronized voltage measurements is presented in [3]. The process can be applied to both transposed and untransposed lines but requires source impedance data. Also, fault distance calculation results indicate the dependence on the type of fault and the fault resistance involved. Generally, the percentage error in distance calculation increases with higher fault resistance.

Fault location algorithms for two-terminal systems using unsynchronized data measurements are presented in [9–11]. An iterative procedure is developed in [9] where the unknown synchronization angle can be found using the Newton–Raphson technique. A similar iterative procedure is presented in [11] where a modified secant method is used to obtain the value of the unknown

* Corresponding author. Tel.: +971 65152556.
E-mail address: aosmanahmed@aus.edu (A.H. Osman).

http://dx.doi.org/10.1016/j.ijepes.2015.11.060
0142-0615/

synchronization angle. In [10], a non-iterative fault location and synchronization procedure is developed by using incremental positive sequence quantities for symmetrical faults, and simultaneously using positive and negative sequence quantities for unsymmetrical faults. All of the procedures presented in [9–11] result in multiple pairs of synchronization angle and fault distance values. The multiple solutions must be carefully treated with specially developed conditions to select the correct pair of angle and distance.

The PMU-based fault location schemes provide the advantage of being insusceptible to source impedance behind the relay, fault resistance involved and any remote in-feed from far end terminals [15]. However, the fact remains that GPS assisted PMUs are still not as widely adopted as they could be due to economic considerations. Therefore, data obtained from asynchronous fault recorders need to be corrected by using a complex synchronization operator ($e^{j\delta}$), where δ is the synchronization angle. Moreover, the application of two-end fault location algorithms on multi-terminal lines would require $2n$ fault data recorders, where n is the number of system terminals.

In this paper, a simple alternative offline-stage fault location algorithm is developed using unsynchronized measurements from one fault data recorder placed on each terminal bus as shown in Fig. 1. The multi-terminal system used in this paper is a four generator EHV system with five transmission lines that need to be protected. The basic principles of two and three-terminal line protection are extended to a multi-terminal system such as the one shown in Fig. 1 while devising the proposed algorithm. The distributed parameter line model is strictly used to represent high voltage transmission lines such that their behaviors resemble real-world system dynamics.

A non-iterative data synchronization procedure is proposed using known pre-fault measurements. Data synchronization can be carried out in a single-shot fashion without any constraints on the amount of synchronization required by the system. Different from the algorithms presented in [9–11], the proposed data synchronization procedure, presented in section 'Data synchronization and faulted leg identification procedure', provides the additional advantage of working as a faulted leg identification method as well. Therefore, there is no need for Clarke transformation based detection methods as described in [1–3]. Section 'Fault location scheme' presents the fault location formulation for the four-terminal system used in the paper. The formulation results in five distance functions, one for each line, which not only identify the faulted leg but also clearly point out the correct tee-point, are given in section 'Algorithm evaluation'.

Data synchronization and faulted leg identification procedure

The multi-terminal system of Fig. 1 is assumed to have a fault data recorder placed on each terminal bus. The synchronization procedure begins with the designation of one of the terminal buses as the common reference point. In this case, bus 4 is used as the common reference. The technique is designed such that data from other ends can be synchronized without any restriction on the amount of synchronization needed by the system before the fault location process can be initiated. Thus, the synchronization procedure works for both acute and obtuse synchronization angles. The various types of faults differ in the type of sequence component quantities present in voltages and currents during faulted operation. Of all the different fault types, the presence of positive sequence quantities is common for both symmetrical and non-symmetrical faults. Therefore, only positive sequence phasors are used for the data synchronization process and fault location scheme. It should also be noted that the synchronization procedure developed in this section is suitable for implementation on a digital micro-processor.

Data synchronization

Once the three-phase quantities are decoupled using symmetrical component transformation, the relationship between positive sequence voltage and current at location x from any bus can be expressed as [11]:

$$\frac{\partial V_1}{\partial x} = Z_1 I_1$$
$$\frac{\partial I_1}{\partial x} = Y_1 V_1 \quad (1)$$

where V_1 and I_1 are the positive sequence voltage and current, respectively, Z_1 is the positive sequence impedance and Y_1 is the positive sequence admittance.

The solution of the above two decoupled equations can be written in a two port network form by applying the boundary conditions as follows:

$$\begin{bmatrix} V_{s1} \\ I_{s1} \end{bmatrix} = \begin{bmatrix} \cosh(\gamma_1 l) & Z_{c1}\sinh(\gamma_1 l) \\ \sinh(\gamma_1 l)/Z_{c1} & \cosh(\gamma_1 l) \end{bmatrix} \begin{bmatrix} V_{R1} \\ I_{R1} \end{bmatrix} \quad (2)$$

where V_{S1} and I_{S1} are the positive sequence voltage and currents at the sending end, respectively, and V_{R1} and I_{R1} are the positive sequence voltage and current at the receiving end, respectively. γ_1 is the positive sequence propagation constant and l is the line length.

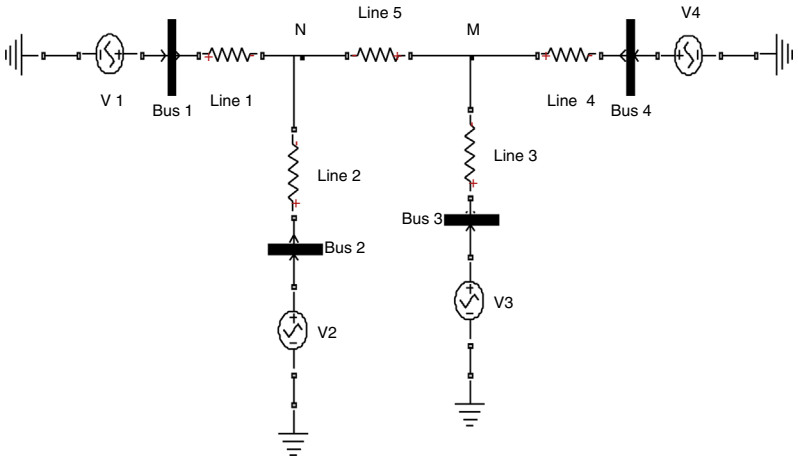

Fig. 1. Multi-terminal system.

It is helpful to express (2) in terms of the sending end quantities to calculate the voltage and current at any distance x from line terminal.

$$\begin{bmatrix} V_{x1} \\ I_{x1} \end{bmatrix} = \begin{bmatrix} \cosh(\gamma_1 x) & -Z_{c1}\sinh(\gamma_1 x) \\ -\sinh(\gamma_1 x)/Z_{c1} & \cosh(\gamma_1 x) \end{bmatrix} \begin{bmatrix} V_{s1} \\ I_{s1} \end{bmatrix} \tag{3}$$

The voltage and current phasors calculated from data measurement at buses 1, 2 and 3 need to be corrected by using the synchronization operator [9–11]:

$$V_{n1} = V_{n1} e^{j\delta_n} \tag{4a}$$

$$I_{n1} = I_{n1} e^{j\delta_n} \tag{4b}$$

where V_{n1} and I_{n1} are the positive sequence voltage and current measured at bus n, respectively and δ_n is the synchronization required for bus n.

Using (3) and (4), the pre-fault positive sequence voltage and current phasors of bus 3 at the tee-point M results in the following expression:

$$V_M^+ = V_{31} e^{j\delta_3} \cosh(\gamma_1 L_3) - I_{31} e^{j\delta_3} Z_{c1} \sinh(\gamma_1 L_3) \tag{5a}$$

$$I_M^+ = -V_{31} e^{j\delta_3} \sinh(\gamma_1 L_3) \frac{1}{Z_{c1}} + I_{31} e^{j\delta_3} \cosh(\gamma_1 L_3) \tag{5b}$$

The projected voltage and current at the tee-point M using the reference bus (bus 4) voltage and current are:

$$V_M^+ = V_{41} \cosh(\gamma_1 L_4) - I_{41} Z_{c1} \sinh(\gamma_1 L_4) \tag{6a}$$

$$I_M^+ = -V_{41} \sinh(\gamma_1 L_4) \frac{1}{Z_{c1}} + I_{41} \cosh(\gamma_1 L_4) \tag{6b}$$

In general, V_{x1} and I_{x1} represent the positive sequence voltage and current at bus x, respectively. V_T^+ and I_T^+ represent positive sequence voltage and current at tee-point M or N, respectively. L_x represents line x length.

By adding (5b) and (6b), the total current at tee-point M from buses 3 and 4 can be expressed as:

$$\begin{aligned} I_{M(3,4)}^+ = {} & -V_{31} e^{j\delta_3} \sinh(\gamma_1 L_3) \frac{1}{Z_{c1}} + I_{31} e^{j\delta_3} \cosh(\gamma_1 L_3) \\ & - V_{41} \sinh(\gamma_1 L_4) \frac{1}{Z_{c1}} + I_{41} \cosh(\gamma_1 L_4) \end{aligned} \tag{7}$$

Using the expressions for the positive sequence voltage and current at the tee-point M in (6a) and (7), the positive sequence voltage at the tee-point N can be calculated using the two-port network equation in (3).

$$V_N^+ = V_M^+ \cosh(\gamma L_5) - I_{M(3,4)}^+ Z_{c1} \sinh(\gamma L_5) \tag{8}$$

The positive sequence voltage at tee-point N in (8) is also equal to the voltage projected from buses 1 and 2. This can be expressed as:

$$\begin{aligned} V_N^+ &= V_{11} e^{j\delta_1} \cosh(\gamma L_1) - I_{11} e^{j\delta_1} Z_{c1} \sinh(\gamma L_1) \\ &= V_M^+ \cosh(\gamma L_5) - I_{M(3,4)}^+ Z_{c1} \sinh(\gamma L_5) \end{aligned} \tag{9}$$

$$\begin{aligned} V_N^+ &= V_{21} e^{j\delta_2} \cosh(\gamma L_2) - I_{21} e^{j\delta_2} Z_{c1} \sinh(\gamma L_2) \\ &= V_M^+ \cosh(\gamma L_5) - I_{M(3,4)}^+ Z_{c1} \sinh(\gamma L_5) \end{aligned} \tag{10}$$

With some mathematical manipulation, expressions in (5a), (9) and (10) can be re-arranged and expressed in a concise matrix form as shown below:

$$e^{j\delta_3}[M_{13}] = b_1 \tag{11}$$

$$e^{j\delta_2}[M_{22}] + e^{j\delta_3}[M_{23}] = b_2 \tag{12}$$

$$e^{j\delta_1}[M_{31}] + e^{j\delta_3}[M_{33}] = b_3 \tag{13}$$

where

$$M_{13} = V_{31}\cosh(\gamma_1 L_3) - I_{31} Z_{c1} \sinh(\gamma_1 L_3)$$
$$M_{22} = -V_{21}\cosh(\gamma_1 L_2) + I_{21} Z_{c1} \sinh(\gamma_1 L_2)$$
$$M_{23} = V_{31}\sinh(\gamma_1 L_3)\sinh(\gamma_1 L_5) - I_{31} Z_{c1} \sinh(\gamma_1 L_5)\cosh(\gamma_1 L_3)$$
$$M_{31} = -V_{11}\cosh(\gamma_1 L_1) + I_{11} Z_{c1} \sinh(\gamma_1 L_1)$$
$$M_{33} = V_{31}\sinh(\gamma_1 L_3)\sinh(\gamma_1 L_5) - I_{31} Z_{c1} \sinh(\gamma_1 L_5)\cosh(\gamma_1 L_3) \text{ and,}$$
$$b_1 = V_{41}\cosh(\gamma_1 L_4) - I_{41} Z_{c1} \sinh(\gamma_1 L_4)$$
$$b_2 = -V_{41}\cosh(\gamma_1 L_4)\cosh(\gamma_1 L_5) + I_4 Z_{c1} \sinh(\gamma_1 L_4)\cosh(\gamma_1 L_5) - V_4 \sinh(\gamma_1 L_4)\sinh(\gamma_1 L_5) + I_4 Z_{c1}\cosh(\gamma_1 L_4)\sinh(\gamma_1 L_5)$$
$$b_3 = b_2$$

Eqs. (11)–(13) can now be expressed as:

$$\begin{bmatrix} M_{11} & M_{12} & M_{13} \\ M_{21} & M_{22} & M_{23} \\ M_{31} & M_{32} & M_{33} \end{bmatrix} \begin{bmatrix} e^{j\delta_1} \\ e^{j\delta_2} \\ e^{j\delta_3} \end{bmatrix} = \begin{bmatrix} b_1 \\ b_2 \\ b_3 \end{bmatrix} \tag{14}$$

where

$$M_{11} = M_{12} = M_{21} = M_{32} = 0$$

The synchronization angle vector δ, required for synchronizing data measured at buses 1, 2 and 3 with respect to bus 4, can now be calculated from (14) and is given by the following expression:

$$\delta^\circ = \begin{bmatrix} \delta_1 \\ \delta_2 \\ \delta_3 \end{bmatrix} = Arg\left(\begin{bmatrix} M_{11} & M_{12} & M_{13} \\ M_{21} & M_{22} & M_{23} \\ M_{31} & M_{32} & M_{33} \end{bmatrix}^{-1} \begin{bmatrix} b_1 \\ b_2 \\ b_3 \end{bmatrix} \right) \times \frac{pi}{180} \tag{15}$$

where the angle vector δ is in degrees as given in (15). The required synchronization angles can be obtained for each incoming voltage and current data sample after calculating the positive sequence phasors. Eq. (15) makes it possible to calculate all the required synchronization angles at once and it is convenient for implementation on a digital computer.

The data synchronization procedure proposed in this section can be further extrapolated and applied to a generalized N-terminal system shown in Fig. 2. Signal synchronization required for the Nth terminal can be calculated by equating the projected voltages of the reference bus, V_s, and the line terminal voltage, V_n, at the tie-in point T_n. This would result in an N-dimensional system of equations similar to that derived in (15) and can be solved for the required synchronization angle vector.

Faulted leg identification

The fault detection schemes described in [1,2] utilize Clarke transformation of inter-phase signals to obtain the decoupled ground and aerial mode quantities. In those schemes, a fault detection index is formulated and used with a threshold to detect the faulted leg in the teed system. The fault detection scheme described in [3] evaluates each bus voltage at the tee-point to observe any large differences that indicate a faulted leg. In this work, a faulted leg identification scheme is developed to work along with the fault location algorithm. The scheme of the faulted leg identification is inherent in the data synchronization process.

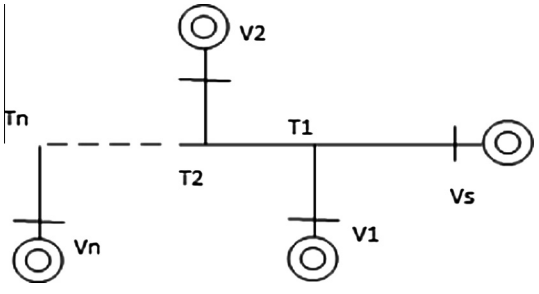

Fig. 2. Generalized N-terminal system.

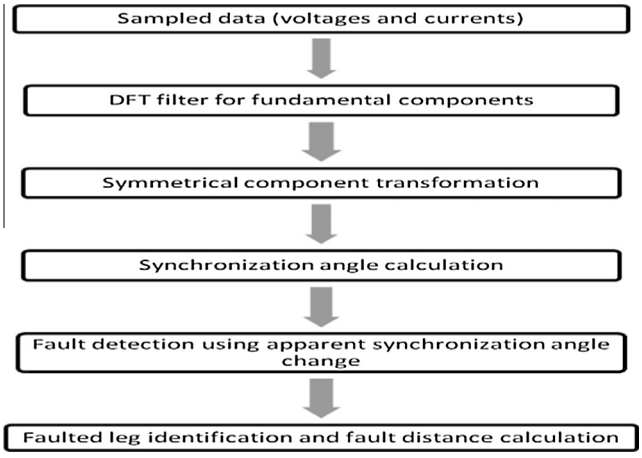

Fig. 3. Fault locator algorithm.

An overview of the complete algorithm at various stages is shown in Fig. 3. The system calculates and records the synchronization angle during the steady-state pre-fault condition. Once a fault occurs on any of the five protected transmission lines, Eq. (15) gives the deviation from the steady state synchronization angle values. This deviation is used to determine whether a particular terminal is operating under a fault condition. The detection of fault on any of the legs is formalized in the following pseudo-code:

if $|\delta(t) - \delta_{steady\text{-}state}| \geqslant threshold$
then
locate fault

The fault location and faulted-leg identification scheme will be described in the following section. This scheme is immune to power system transients such as abrupt load switching. As a safety measure, the algorithm registers a fault condition only if the synchronization angle deviation of 0.1° persists for more than three consecutive data samples. The use of this scheme obviates the need for carrying out system decoupling using Clarke transformation and responds correctly over a large variation of fault resistance.

Fault location scheme

The fault location scheme involves reducing the multi-terminal system to a two-terminal system such that the faulted leg is contained in the reduced two-terminal line. The fault location function developed here is applied to a 4-terminal system that has a phase-to-ground fault on line 1 as shown in Fig. 4. Positive sequence voltage and current phasors are used to ensure that the scheme can work for other fault types as well.

To reduce the four-terminal system that contains a faulted leg to a two-terminal one, the total current entering the tee-point (N) and its voltage have to be calculated. The voltage at N is given by (8) and the total current entering N is given by the following expression:

$$I_N^+ = -\frac{V_M^+ \sinh(\gamma_1 L_5)}{Z_{c1}} + I_{M(3,4)}^+ \cosh(\gamma_1 L_5) - V_{21} e^{j\delta_2} \frac{\sinh(\gamma_1 L_2)}{Z_{c1}} + I_{21} e^{j\delta_2} \cosh(\gamma_1 L_2) \quad (16)$$

where I_N^+ is the positive sequence current entering N. Using (8) and (16), let:

$$A_1 = V_N^+$$
$$B_1 = I_N^+$$

The voltage at the fault point is given by the following two equations:

$$V_{F1} = A_1 \cosh(\gamma_1 L_1 (1 - d_1)) - B_1 Z_{c1} \sinh(\gamma_1 L_1 (1 - d_1)) \quad (17)$$

$$V_{F1} = V_{11} e^{j\delta_1} \cosh(\gamma_1 L_1 d_1) - I_{11} e^{j\delta_1} Z_{c1} \sinh(\gamma_1 L_1 d_1) \quad (18)$$

where d_1 is the per-unit distance to the fault point from bus 1.

Subtracting (18) from (17) and rearranging gives the expression for the per-unit distance to the fault point.

$$d = \frac{arctanh\left(\frac{A_1 \cosh(\gamma_1 L_1) - B_1 Z_{c1} \sinh(\gamma_1 L_1) - V_{11} e^{j\delta_1}}{-I_{11} e^{j\delta_1} Z_{c1} + A_1 \sinh(\gamma_1 L_1) - B_1 Z_{c1} \cosh(\gamma_1 L_1)}\right)}{\gamma_1 L_1} \quad (19)$$

Using the synchronization operator calculated during steady-state, the per-unit complex valued distance to the fault point can be calculated using (19). Using similar reductions, distance functions for the other four transmission lines can also be derived which would result in a total of five distance functions. The distance functions are evaluated once the faulted leg identification scheme described in the previous section detects a fault condition. Evaluating the five distance functions will result in one function yielding a per unit value less than 1, which helps to single out the faulted transmission line. The pseudo-code for identifying the faulted leg is shown below:

if
$d_i < 1$
then
faulted line $= i$

where d_i is the distance function for line i.

For faults on the tee-point M, d_3, d_4 and d_5 will indicate a per unit value of 1. Whereas for a fault on the tee-point N, d_5 will indicate a per unit value of zero.

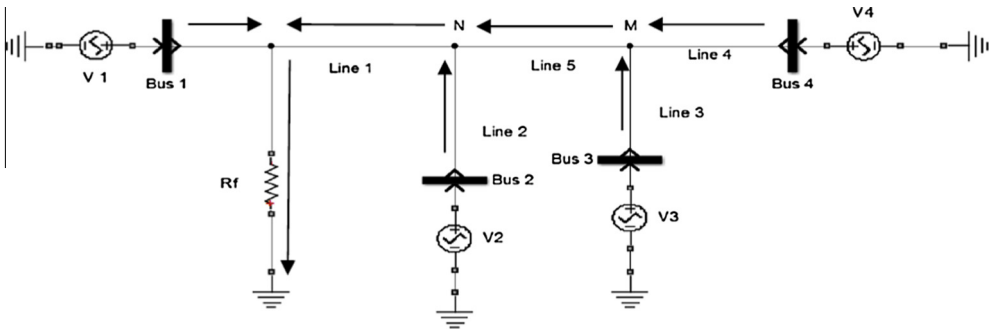

Fig. 4. Fault on line 1 with assumed current directions.

Algorithm evaluation

The four-terminal line system shown in Fig. 1 is modeled using Matlab/Sim-Power-System toolbox. The parameters of the transmission lines and their lengths are shown in Tables 1 and 2, respectively. The system is supplied by 735 kV sources at different angles as shown in Table 3. The proposed multi-terminal fault location algorithm using unsynchronized measurements is evaluated in the following subsection.

Synchronization, fault detection and location

The signals obtained from Matlab/Sim-Power-System simulations are naturally synchronized. In order to evaluate the performance of the proposed algorithm, the signals obtained from buses 1, 2 and 3 were delayed by 96°, 30° and 45°, respectively. Signals from bus 1 was delayed by 96° to show that the algorithm works for large synchronization angles as well.

The calculated synchronization angles during steady-state operation, using (15), are shown in Fig. 5. It is obvious that the proposed algorithm is able to accurately reveal the synchronization angles. A single-phase-to-ground fault is applied on line 1 at 0.1 s. The apparent deviation of synchronization angles from their steady state value is shown in Fig. 6. The results show that the deviation of the synchronization angle from the steady-state value of line 1 exceeds the threshold, and thus a fault is detected on this line. Fig. 7 depicts the real and imaginary components of the fault distance estimate for line 1.

The fault distance functions derived in the previous section were run concurrently to yield distance estimates for each of the transmission lines as shown in Fig. 8. With the fault placed on line 1, all the distance functions with the exception of line 5 report a per-unit value which violates the criterion described in section 'Fault location scheme' for identifying the faulted leg. An apparently peculiar feature of the distance function derived for transmission line 5 is that it yields a per-unit solution of 0 when short-circuit faults occur to the left of its reference terminal as shown

Table 1
Line impedance parameters.

Parameter	Positive sequence (km)	Zero sequence (km)
R	0.011223	0.30079
L	0.00086848	0.002988
C	1.34E−08	8.59E−09

Table 2
Line lengths.

Line	Length (km)
1	100
2	140
3	180
4	200
5	50

Table 3
Angels of voltage sources.

Source	Angle (°)
1	15
2	10
3	5
4	0

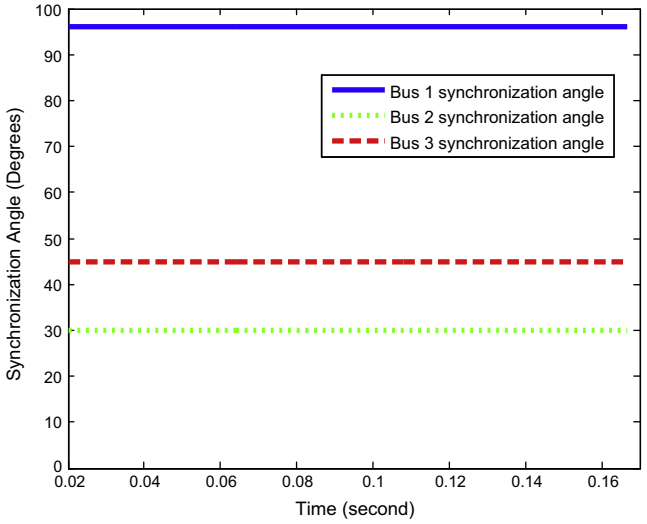

Fig. 5. Calculated synchronization angle.

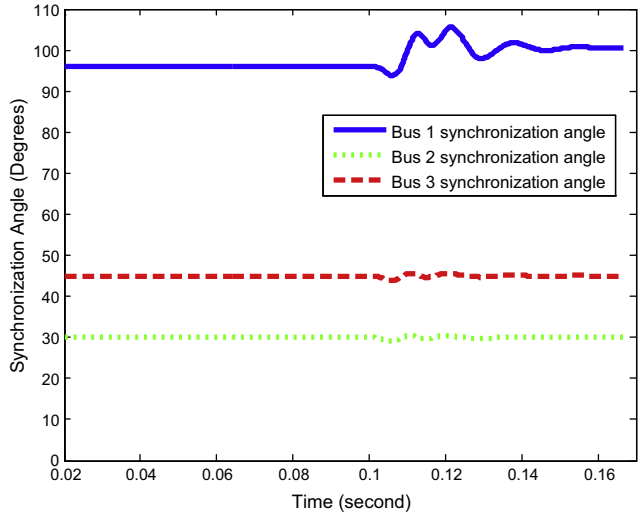

Fig. 6. Apparent deviation of synchronization angles.

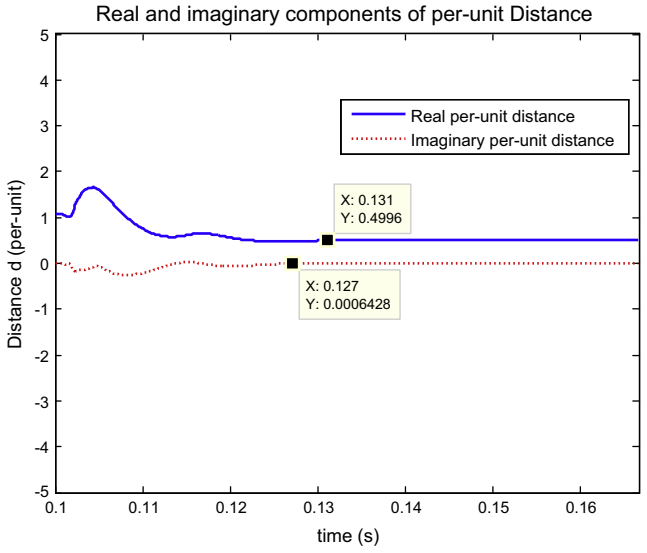

Fig. 7. Per-unit distance to fault.

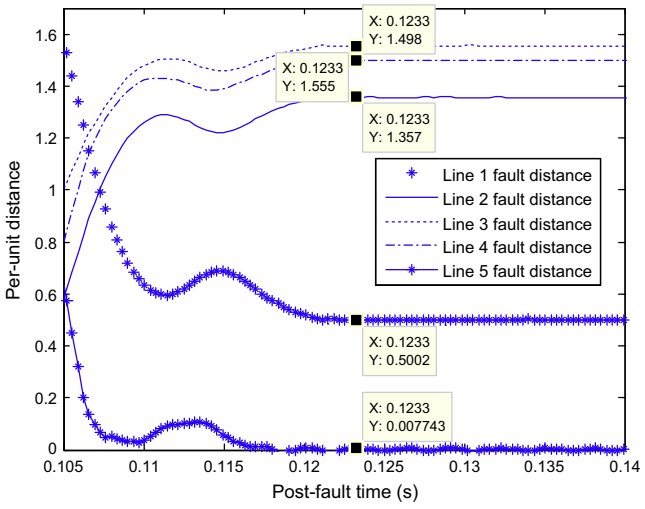

Fig. 8. Per-unit fault distance estimates of all lines.

Table 4
Performance of fault location scheme.

Faulted line	Fault			% Error
	Type	Location	R_F (Ω)	
Line 1	AG	10% from bus 1	1	0.012
	BC	30% from bus 1	50	0.024
	ABG	50% from bus 1	100	0.015
	ABC	85% from bus 1	200	0.019
Line 2	AG	10% from bus 2	1	0.045
	BC	30% from bus 2	50	0.031
	ABG	50% from bus 2	100	0.014
	ABC	85% from bus 2	200	0.016
Line 3	AG	10% from bus 3	1	0.041
	BC	30% from bus 3	50	0.019
	ABG	50% from bus 3	100	0.039
	ABC	85% from bus 3	200	0.028
Line 4	AG	10% from bus 4	1	0.052
	BC	30% from bus 4	50	0.017
	ABG	50% from bus 4	100	0.027
	ABC	85% from bus 4	200	0.021
Line 5	AG	10% from *N*	1	0.021
	BC	30% from *N*	50	0.019
	ABG	50% from *N*	100	0.026
	ABC	85% from *N*	200	0.038

in Fig. 8. Faults occurring at the terminal of line 5 (tee-point *N*) are equivalent to faults placed at a distance of 1 per-unit from the terminal of line 2. Since the per-unit distance to fault for line 2 is not equal to 1 based on Fig. 8, the results from line 5 can be safely discarded which leaves line 1 being correctly identified as the faulted leg. As can be seen in Fig. 8, the algorithm converges to an accurate estimate of fault distance well within two fundamental frequency cycles of the available recorded signals before the operation of the circuit breakers.

Different types of faults with various fault resistances are placed on different sections of the five transmission lines and the percentage error of the fault distance calculation is recorded. As shown in Table 4, different transmission lines are tested with different fault types. The fault resistance is varied from 1 to 200 Ω to cover a large variance. The percentage error for all fault types on transmission lines is well within the 1% margin and do not exhibit any particular trend. In all cases, the algorithm is able to identify the faulted transmission line since the calculated per unit distance was less than 1.0 using the method described earlier in section 'Fault location scheme'.

Power system transients and fault detection

Power systems are often subjected to transients that fade away within the span of a few fundamental power cycles. Studying the response of protective devices to transient conditions is crucial to avoid malfunctioning and false tripping of relays. In this subsection, the security and stability of the developed synchronization procedure is tested during power system transient conditions.

The algorithm presented in this paper was tested with the system subjected to load switching transients. A 50 MVAR capacitive load was attached to bus 1 as shown in Fig. 9 and the fault detection scheme was analyzed for erroneous false-positive response. The attached load was switched on after the fourth power cycle (0.0667 s) and its effect on the voltage and current waveforms measured at bus 1 was observed. Figs. 10 and 11 clearly show the effect of load switching on the voltage and current waveforms at bus 1, respectively.

The performance of the fault detection scheme is shown in Fig. 12. Despite the waveform distortion, the fault detection scheme is able to correctly ignore the transients without giving a false positive response. The calculated synchronization angles do not show any discernible deviation from their steady state values. The utility of the detection scheme is obvious from the fact that the algorithm was able to distinguish between power system

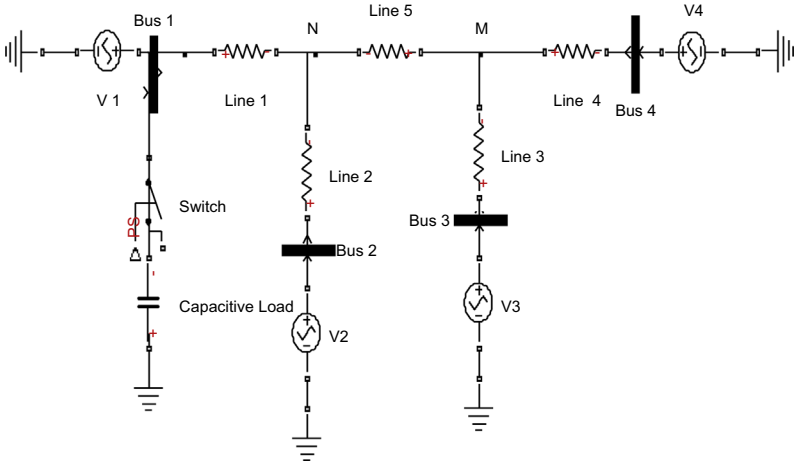

Fig. 9. Multi-terminal line with load.

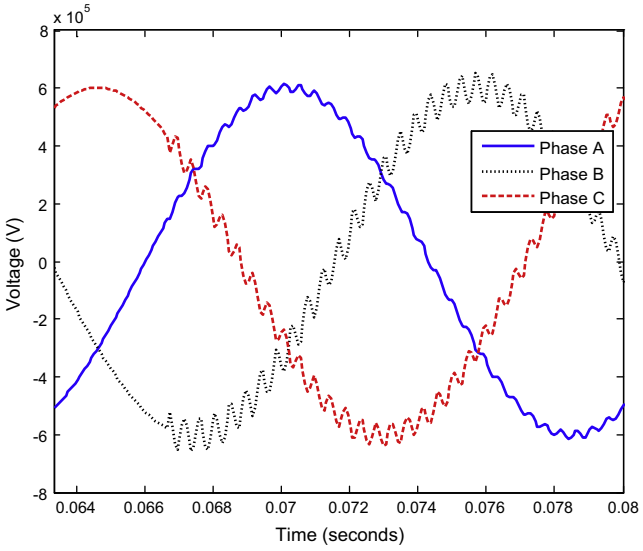

Fig. 10. Bus 1 phase voltage waveforms during transients.

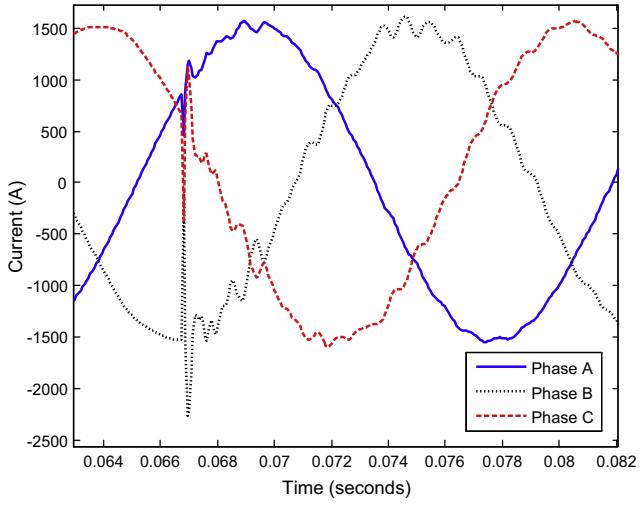

Fig. 11. Bus 1 phase current waveforms during transients.

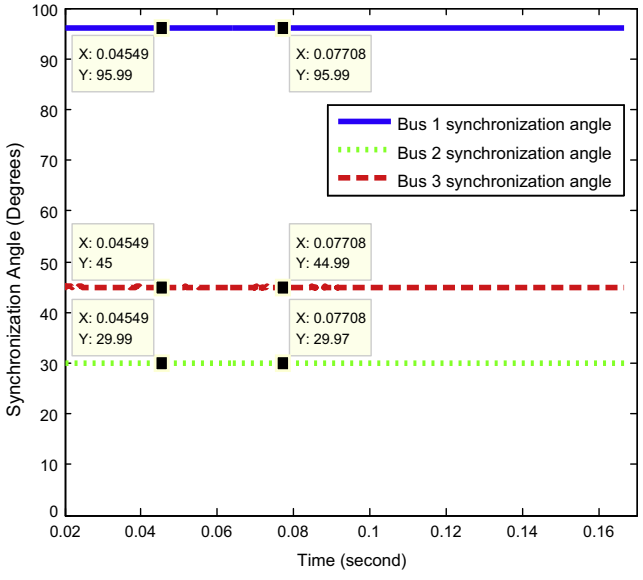

Fig. 12. Synchronization angles during transients.

transients and short circuit faults. The test was successfully repeated with different load levels and by placing the switched load at different buses.

The algorithm was tested more stringently by placing an AB fault with $R_f = 100\ \Omega$ at 50% of line 1 shortly after a load switching transient occurred. The attached load was switched on after cycle number five (0.0833 s), whereas the fault was initiated one cycle later at 0.1 s. The fault location estimate for the test is shown in Table 5 and is consistent with the results shown in the previous subsection.

The current waveforms measured at bus 1 during transients and post-fault are shown in Fig. 13. The synchronization angles calculated during transients and post-fault are shown in Fig. 14. The

Table 5
Fault location estimate after transients.

Faulted line	Fault			% Error
	Type	Location	R_F (Ω)	
Line 1	AB	50% from bus 1	100	0.08

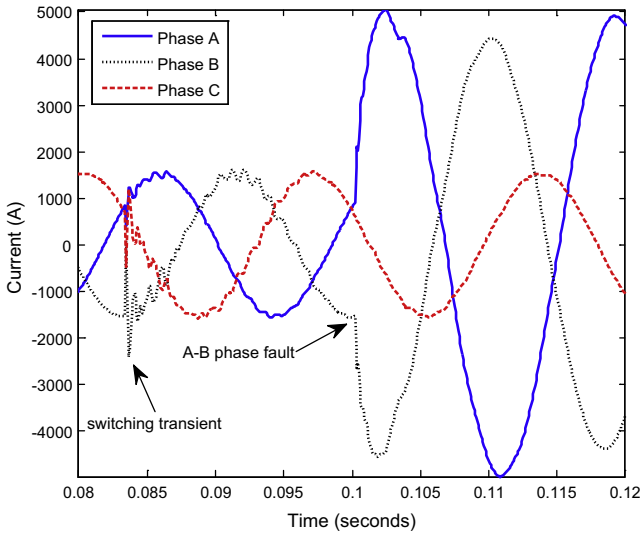

Fig. 13. Bus 1 phase currents waveform during transients and fault.

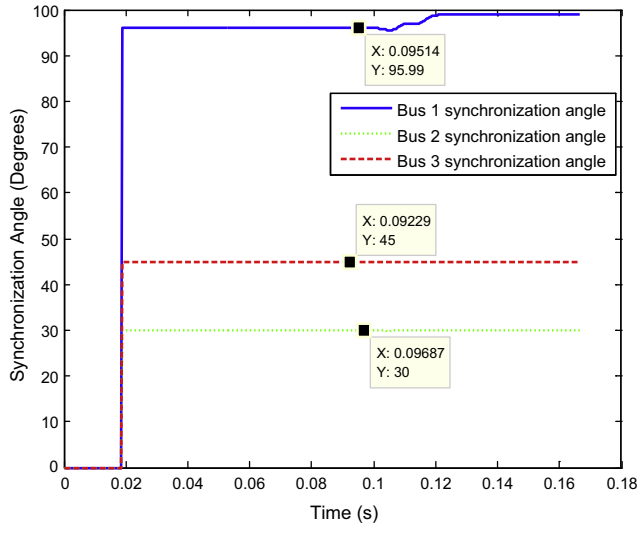

Fig. 14. Synchronization angles during transients and fault.

fault detection scheme was able to successfully differentiate and identify the fault that was placed just one power cycle after initializing switching transients on line 1. This can show the robustness of the proposed algorithm.

Conclusion

This paper proposes an alternative simple faulted leg identification and fault location schemes for multiple-terminal transmission lines which can, in principle, be extended to any *N*-terminal system. The algorithm carries out data synchronization using the known steady-state measurements and utilizes the apparent deviation in synchronization angles to determine a faulted state of operation. The fault location scheme gives accurate estimates for fault distances which are well within the one percent margin. Additionally, the method remains unaffected by power system transients and high fault resistances.

References

[1] Aggarwal RK, Coury DV, Johns AT, Kalam A. A practical approach to accurate fault location on extra high voltage teed feeders. IEEE Trans Power Delivery 1993;8(3):874–83.
[2] Chen Ching-Shan, Liu Chih-Wen, Jiang Joe-Air. Three-terminal transmission line protection using synchronized voltage and current phasor measurements. In: Transmission and distribution conference and exhibition, IEEE/PES Asia Pacific, vol. 3, October 2002. p. 1727–32.
[3] Brahma SM. Fault location scheme for a multi-terminal transmission line using synchronized Voltage measurements. IEEE Trans Power Delivery 2005;20 (2):1325–31.
[4] Chen Ching-Shan, Liu Chih-Wen, Jiang J-A. Application of combined adaptive Fourier filtering technique and fault detector to fast distance protection. IEEE Trans Power Delivery 2006;21(2):619–26.
[5] Yu Chi-Shan. A discrete Fourier transform-based adaptive mimic phasor estimator for distance relaying applications. IEEE Trans Power Delivery 2006;21(4):1836–46.
[6] Ha Heng-xu, Zhang Bao-hui, Yuan Wen-guang, Li Wei-shuo. Novel algorithm of variable-window Fourier transform based high-speed distance relay for EHV transmission lines. In: International Conference on Power System Technology, Power Con 2004, vol. 1, November 2004. p. 6–11.
[7] Osman AH, Abdelazim T, Malik OP. Transmission line distance relaying using on-line trained neural networks. IEEE Trans Power Delivery 2005;20 (2):1257–64.
[8] Brahma SM. New fault location scheme for a two- terminal transmission line using synchronized phasor measurements. In: Transmission and distribution conference and exhibition, 2005/2006 IEEE PES, May 2006. p. 853–7.
[9] Izykowski J, Molag R, Rosolowski E, Saha MM. Accurate location of faults on power transmission lines with use of two-end unsynchronized measurements. IEEE Trans Power Delivery 2006;21(2):627–33.
[10] Izykowski J, Rosolowski E. Accurate non-iterative fault location algorithm for three-terminal line. In: International conference on electrical and electronics engineering, 2009, ELECO 2009, 5–8 November 2009. p. I-154–I-158.
[11] Yu Chi-Shan. An unsynchronized measurements correction method for two-terminal fault-location problems. IEEE Trans Power Delivery 2010;25 (3):1325–33.
[12] Hussain Shoaib, Osman AH. Fault location on series and shunt compensated lines using unsynchronized measurements. Electr Power Syst Res 2014;116:166–73.
[13] Dalcastagne AL, Filho SN, Zurn HH, Seara R. An iterative two-terminal fault-location method based on unsynchronized phasors. IEEE Trans Power Delivery 2008;23(4):2318–29.
[14] Kizilcay M, La Seta P. A new unsynchronized two-terminals fault location method on series compensated lines. In: Power Tech, 2005 IEEE Russia, 27–30 June 2005. p. 1–7.
[15] Esmaeilian A, Mohseninezhad M, Doostizadeh M, Khanabadi M. A precise PMU based fault location method for multi terminal transmission line using voltage and current measurement. In: 10th international conference on environment and electrical engineering (EEEIC 2011), May 2011. p. 1–4.